SPATIAL MAPPING OF BACKGROUND IONIZING RADIATION AND HEAVY METAL CONTAMINATION: AN INTEGRATED RADIOLOGICAL AND TOXICOLOGICAL RISK ASSESSMENT OF SOIL SAMPLES AROUND THE ARIARIA WASTE DUMPSITE, NIGERIA

Gbarato, O. L.
Department of Physics
Ignatius Ajuru University of Education
Rivers State, Nigeria.
oliver.gbarato@iaue.edu.ng

Abstract

Uncontrolled waste dumpsites in rapidly urbanizing regions are complex environmental systems where chemical and radiological hazards coexist but are often assessed separately, limiting understanding of cumulative exposure and long-term health risks. This study presents an integrated spatial assessment of background ionizing radiation (BIR) and heavy metal contamination in soils around the Ariaria waste dumpsite, Nigeria, with the aim of developing a unified radiological–toxicological risk framework. In situ gamma radiation measurements were conducted using a calibrated Geiger–Müller survey meter, while soil samples were analysed for elemental composition using X-ray fluorescence spectrometry. Radiological indices, including absorbed dose rate, annual effective dose equivalent (AEDE), and excess lifetime cancer risk (ELCR), were calculated using standard models. Heavy metal concentrations were evaluated against international guideline limits, and spatial patterns were analysed to identify contamination variability. Results show that the mean absorbed dose (≈193.3 nGy h^{-1}) exceeds the global average of 89 nGy h^{-1}, indicating enhanced radiation from radionuclide-bearing wastes. Although AEDE (≈0.30 mSv y^{-1}) remains within recommended public exposure limits, ELCR (≈1.03 × 10^{-3}) exceeds global reference values, suggesting elevated long-term cancer risk. Geochemical analysis reveals that chromium, uranium, thorium, nickel, and cobalt exceed regulatory thresholds, while cadmium, lead, zinc, and arsenic remain within permissible limits. Spatial patterns indicate heterogeneous contamination driven by waste composition and subsurface processes. Overall, the co-occurrence of radiological and chemical contaminants highlights a chronic, multi-pathway exposure scenario with potential long-term health implications. These findings emphasize the need for integrated monitoring, improved waste management, and targeted remediation strategies.

Keywords: Background Ionizing Radiation, Heavy Metals, Dumpsite Contamination, Spatial Analysis, Environmental Risk Assessment.

Introduction

Rapid urban population growth, combined with increasing rates of solid waste generation, has created a major environmental and public health challenge, particularly in low- and middle-income countries. Municipal waste generation is rising faster than the development of supporting infrastructure, leaving many cities in Africa, Asia, and Latin America without adequate systems for collection, segregation, and disposal (Kaza et al., 2018; Ferronato and Torretta, 2019). As a result, open and uncontrolled dumpsites remain the dominant waste management option in many urban and peri urban areas, driven by weak regulatory enforcement, limited technical capacity, and financial constraints (Wilson et al., 2015; UN Environment Programme, 2019).

These dumpsites receive a complex mixture of municipal, industrial, medical, and electronic waste, forming chemically heterogeneous pollution sources. Through leachate generation, surface runoff, and wind resuspension, they continuously release contaminants into surrounding soils, groundwater, and the atmosphere (Nanda and Berruti, 2021; Gworek et al.,

2018). Studies across West Africa consistently report elevated concentrations of toxic elements such as cadmium, zinc, copper, and lead in soils near dumpsites compared with background levels (Afon et al., 2017; Oyebamiji et al., 2019; Ilechukwu et al., 2020). These findings highlight the role of unmanaged waste sites as persistent and spatially extensive sources of environmental contamination.

Beyond chemical pollution, dumpsites act as centres of multiple environmental stressors. Elevated microbial loads and pathogenic indicators have been reported in soils and groundwater surrounding waste disposal areas, reflecting the interaction between chemical and biological hazards (Ezeonu et al., 2018; Owamah et al., 2020). This co-occurrence of pollutants has been described as a multi hazard exposure system, where communities experience overlapping risks rather than isolated threats (Landrigan et al., 2018; Prüss Ustün et al., 2019). Such complexity underscores the need for integrated assessment approaches that consider chemical, radiological, and biological pathways together.

Radiological assessments in waste affected environments further support this perspective. Studies in the Niger Delta report measurable gamma radiation levels at dumpsites, with annual effective doses comparable to or slightly above global background values (Abayiga et al., 2024). Similar findings from Ebonyi State show elevated radiological hazard indices and lifetime cancer risks linked to naturally occurring radionuclides coexisting with heavy metal contamination (Echeweozo et al., 2025). Although earlier studies have quantified radionuclides such as ^{226}Ra, ^{232}Th, and ^{40}K alongside heavy metals in industrial areas like Sango Ota, most investigations still treat these hazards independently (Ademola et al., 2014).

Heavy metal contamination around dumpsites is equally well documented. Soil and groundwater studies across Nigeria report elevated levels of lead, cadmium, chromium, and zinc above regulatory thresholds, largely driven by leachate migration and seasonal variability (Ugwuaji et al., 2015; Ezeonu et al., 2023). Groundwater contamination is of particular concern, as mobilized metals can infiltrate shallow aquifers and increase both carcinogenic and non-carcinogenic risks, especially among vulnerable populations (Adeleke et al., 2024).

Despite this growing body of evidence, most studies remain narrowly focused on either radiological or chemical contamination. This fragmented approach underestimates cumulative exposure and limits the development of effective remediation strategies. There is a clear need for spatially integrated frameworks capable of capturing the combined distribution and interaction of multiple pollutants.

This study addresses that gap through a unified geospatial assessment of the Osisioma dumpsite. It maps the spatial distribution of background radiation and heavy metals, evaluates their co-occurrence, and develops a cumulative risk framework that reflects combined environmental exposure.

Physics-Based Foundations of Radiological and Toxicological Contamination from Waste Systems

Uncontrolled waste dumpsites are best understood as dynamic environmental systems rather than static accumulations of refuse. Within these environments, physical degradation, chemical reactions, microbial activity, and radioactive decay occur simultaneously, generating multiple and interacting hazards. Waste streams commonly include construction debris, industrial residues, and electronic components that contain both naturally occurring radionuclides and heavy metals. As radionuclides undergo decay, they emit ionizing radiation, while heavy metals are progressively mobilized through rainwater infiltration, dissolution processes, and shifts in soil pH and redox conditions.

These processes highlight a fundamental point: background ionizing radiation and heavy metal contamination are not independent phenomena. They originate from similar waste sources

and are governed by shared subsurface conditions, reinforcing the need for integrated assessment approaches (Kosson et al., 2014; UNSCEAR, 2016).

(i) Radionuclides in Waste

Radionuclides such as ^{226}Ra, ^{232}Th, and ^{40}K are widespread in waste materials and contribute to environmental radiation through radioactive decay, expressed as

$$A = \lambda N \quad (1)$$

where λ is the decay constant and N is the number of radioactive nuclei. Specific activity (Bq kg^{-1}) thus depends on both isotopic abundance and waste composition (UNSCEAR, 2016).

In heterogeneous dumpsites, radionuclides are irregularly distributed within mixed waste layers. Their emitted radiation is attenuated as it passes through surrounding materials according to

$$I = I_0 e^{-\mu x} \quad (2)$$

where I_0 is the unattenuated intensity, μ is the linear attenuation coefficient, and x is the effective path length through waste or soil (IAEA, 2018). Ongoing waste degradation alters material density and structure, producing spatially variable radiation fields. As waste degrades physically and chemically over time, void formation and material settling alter both radionuclide distribution and radiation escape pathways, leading to spatially variable BIR fields around dumpsites.

(ii) Heavy Metal Mobilisation and Physico-Chemical Leaching Processes

Similarly, unmanaged dumpsites serve as long-term sources of heavy metals including lead, cadmium, chromium, nickel, copper, and zinc. These elements are commonly present in discarded batteries, metal scraps, electronic components, pigments, treated wood, and industrial residues. Their release into the surrounding environment does not occur instantaneously but unfolds gradually through the formation of leachate, a chemically reactive liquid generated when rainwater infiltrates waste layers and percolates downward. In essence, infiltrating water acts as a solvent, extracting soluble constituents from decomposing waste and transporting them into surrounding soils and groundwater (Kosson et al., 2014; Christensen et al., 2011).

Leachate chemistry evolves as the waste mass ages. In the early stages of waste decomposition, microbial degradation of organic matter produces acidic conditions, lowering pH and enhancing the solubility of many metals. Over time, as methanogenic conditions develop, the system often shifts toward near-neutral or mildly alkaline pH. Throughout this progression, the mobility of metals is strongly influenced by redox potential, which controls their oxidation state and therefore their solubility and toxicity. For example, chromium may exist in the less mobile Cr(III) form under reducing conditions or the highly mobile and more toxic Cr(VI) form under oxidizing conditions (Christensen et al., 2011; ATSDR, 2012).

In addition, dissolved organic carbon, chloride, sulfate, and carbonate ions can form complexes with metal ions, increasing their solubility and enhancing their transport potential. Ionic strength and microbial processes further modify metal partitioning between solid and liquid phases. As a result, metals are mobilized through a combination of dissolution from solid waste particles, desorption from mineral surfaces, and complexation in the aqueous phase. Conceptually, this can be represented as a dynamic equilibrium between solid-bound metals and dissolved ionic species, mediated by pH, redox conditions, and ligand availability (Kosson et al., 2014; Alloway, 2013). Metal mobilization occurs via dissolution, desorption, and complexation**,** which may be expressed conceptually as:

$$M_{solid} \rightleftarrows M^{n+}_{aqueous} + liquids \quad (3)$$

Frameworks such as the Leaching Environmental Assessment Framework demonstrate that contaminant release is governed by environmental conditions rather than occurring randomly (Kosson et al., 2014).

Importantly, the same processes that drive metal leaching can also enhance radionuclide mobility. This shared geochemical behaviour provides a clear basis for the co release and migration of chemical and radiological contaminants.

(iii) Gamma Radiation Propagation and BIR Spatial Footprints

Gamma radiation propagation around waste disposal sites describes how energetic photons travel through the air and the ground around this site. Gamma rays do not simply stay where they are emitted. Instead, they move outward and are gradually reduced in intensity the farther they travel. This behaviour can be described mathematically by an exponential attenuation relationship based on Beer's Law using the equation

$$I(r) = I_0 \exp(-\mu r) \quad (4)$$

Here I(r) is the intensity of gamma radiation at a distance r, I_0 is the intensity at the source, and μ is a material-specific attenuation coefficient that reflects how readily the surrounding medium (air, soil, moisture) absorbs or scatters gamma photons. In practice there is also geometric spreading as photons travel outward from a point source, which further reduces measured intensity with distance (Knoll, 2010; IAEA, 2018).

During measurements radiation dose rates in the environment, measurements are taken at a single microscopic point. Instead, most instruments, whether handheld survey meters, airborne sensors, or vehicle-mounted spectrometers, receive radiation from a three-dimensional volume of soil and air around the detector. The effective area contributing to the measurement is often called the spatial footprint. At typical detector heights above the ground, this footprint can extend tens of metres in all directions, with the size and shape depending on photon energy, detector geometry, and how strongly the soil beneath the sensor attenuates gamma photons (IAEA, 2018; McLaughlin et al., 2013).

Soil physical properties themselves also influence what is measured. Moisture and bulk density affect where radioactive elements reside and how tightly they are bound to soil particles, but they also change how gamma photons travel. Water and dense soil have more electrons per unit volume, which increases gamma attenuation compared with dry, loose material. That means wetter or denser patches of soil reduce the gamma signal more strongly than dry or porous patches. As a result, maps of background ionising radiation (BIR) do not reflect just the amount of radioactive material present**.** They also reflect physical variations in the ground, such as changes in moisture, texture and compaction. Because these subsurface conditions are rarely uniform, radiation fields measured over dumpsites tend to be spatially heterogeneous, with "hotter" and "cooler" areas that arise from both radiological and physical factors (UNSCEAR, 2016; IAEA, 2018; Tollefson et al., 2015).

(iv) Heavy Metal Migration in Soil and Groundwater

The movement of heavy metals through soils and groundwater is controlled by a combination of physical and chemical processes that together determine how far and how fast contaminants travel. At the heart of these processes is a transport equation that balances dispersion, flow, and interactions with the solid phase:

$$\frac{\partial C}{\partial t} = D\nabla^2 - v.\nabla C - \frac{\rho_b}{\theta} k_d \frac{\partial C}{\partial t} \quad (5)$$

In this equation, C represents the concentration of a dissolved contaminant, D is the dispersion coefficient that quantifies spreading due to variations in pore water velocity, v is the groundwater velocity described by Darcy's Law, ρ_b is the soil bulk density, θ is the soil porosity, and k_d is the distribution coefficient that captures how strongly the metal adheres to soil particles. The first term on the right side describes mechanical dispersion, which spreads a contaminant plume both along the flow direction and sideways in response to variations in flow

paths at the pore scale. The second term captures advection, the process by which dissolved metals are carried along with the bulk movement of groundwater from areas of higher hydraulic head to lower. When groundwater velocities are very low, molecular diffusion, driven by concentration gradients alone, becomes important in redistributing dissolved metals (Fischer and Kincaid 2014; Zheng and Bennett 2015).

Metal mobility is also profoundly influenced by interactions between the dissolved species and the solid matrix. This process is typically referred to as sorption, and it slows down the apparent movement of contaminants relative to the groundwater itself. The distribution coefficient k_d is a simple measure of the strength of sorption; higher k_d values indicate stronger attachment to soil particles and greater retardation of movement. For example, lead and copper generally have relatively high k_d values and therefore tend to be strongly retained by soils, producing steeper concentration gradients close to the source zone. In contrast, hexavalent chromium and cadmium often remain more mobile under oxidizing conditions because they sorb less strongly and are not easily fixed by mineral surfaces (Bradl 2017; Chen and Wang 2018; Li and Zhang 2016).

These physical and chemical laws do more than just populate equations on a page. When environmental scientists create maps of contaminant plumes using geographic information systems these maps are not just descriptive illustrations. They are direct manifestations of subsurface transport physics. The shape of a plume, its width, and how far it extends from a source reflect the combined effects of groundwater flow, dispersion, diffusion, and sorption processes that occur beneath our feet (Hubbard and Auken, 2015; Zhou et al., 2017). By understanding and quantifying these processes, scientists can more accurately predict contaminant movement and support better remediation and land management decisions.

(v) Radiological Dose Pathway

Gamma radiation in the environment can expose people to ionizing radiation because the energy from gamma photons contributes to an absorbed dose rate in air and tissues. Scientists measure this as D, in units of nanograys per hour (nGy/hr). To understand how this translates into a risk for a person, the absorbed dose must be converted to an effective dose, E, that accounts for how long a person is exposed and how the body responds to that radiation. This relationship is traditionally expressed as:

$$E = \mathrm{D} \times \mathrm{T} \times \mathrm{C_f} \quad (6)$$

In this equation, T, is the amount of time a person spends in the radiation field, and $\mathrm{C_f}$ is a dose conversion coefficient that accounts for the biological effectiveness of the radiation and typical body geometry. For adults, a commonly used conversion coefficient is about 0.7 sieverts per gray. Frameworks developed by organizations such as the United Nations Scientific Committee on the Effects of Atomic Radiation help formalize how environmental measurements of gamma flux are translated into doses that reflect real human behaviour, including where people live, how they move, and how long they stay in different environments (UNSCEAR, 2016; Smith and Jones, 2015; IAEA 2014).

In any environmental study of ionizing radiation, such as around the Osisioma Waste Dumpsite, it is essential to move beyond raw instrument readings to metrics that describe how radiation energy interacts with the human body and what the health implications are**.** Therefore, it is important to introduce other dosimetric quantities used to translate in-situ gamma measurements into meaningful risk estimates, such as absorbed dose rate, equivalent dose, annual effective dose equivalent (AEDE), and excess lifetime cancer risk (ELCR)**.**

(a) Absorbed Dose Rate

Absorbed dose rate quantifies how much ionizing radiation energy is deposited per unit mass in a material (often air or tissue) per unit time. In SI units, the absorbed dose is measured in

grays (Gy), where 1 Gy = 1 joule per kilogram (J kg^{-1}). It expresses the physical energy transfer from gamma photons to matter without reference to biological effect. At a basic physical level, absorbed dose arises from the energy per unit mass deposited by gamma photons as they interact through processes like Compton scattering or photoelectric absorption. The external exposure rate data obtained for BIR levels were used for calculation of the absorbed dose rate $nGyh^{-1}$, using the conversion factor (Raique et al, 2014)

$$1\mu Rh^{-1} = 8.7nGyh^{-1} = 8.7\ x\ 10^{-9}\mu Gy\ x\ 8760y^{-1} = 76.212\mu Gy^{-1} \quad (7)$$

(b) Equivalent Dose

While the absorbed dose describes energy deposited, the equivalent dose accounts for the relative biological effectiveness of different radiation types. This quantity adjusts energy deposition by radiation weighting factors to better reflect the likelihood of biological damage. Therefore, when exposed to ionizing radiation, it is appropriate to evaluate the dose rate to the entire body per year, using the National Council on Radiation Protection (NCRP) recommendation (NCRP, 1993; Avwiri et al, 2013).

$$1.0mRh^{-1} = \frac{0.96\ x\ 24\ x\ 365}{100}\ mSvy^{-1} \quad (8)$$

(c) Annual Effective Dose Equivalent

The annual effective dose equivalent provides this bridge. It begins with the absorbed dose rate in air and then scales it up to reflect exposure over an entire year. Since there are 8760 hours in a year, the measured hourly dose rate is multiplied by total annual time. But that is still not enough, because individuals do not remain continuously in the radiation field. To account for this, an occupancy factor is introduced. For outdoor exposure assessments, a value of 0.2 is often used, meaning that people are assumed to spend about twenty percent of their time outdoors at the measured location. Indoor exposure may use different factors, reflecting different living habits and building shielding characteristics (UNSCEAR, 2016; IAEA, 2014). After adjusting for time, the absorbed dose must also be converted into effective dose. This is achieved using a dose conversion coefficient, commonly 0.7 sieverts per gray for adults exposed to environmental gamma radiation. This coefficient is derived from radiation transport calculations through human phantoms and represents how energy deposited in air translates to dose within human tissues. It integrates anatomical geometry, photon energy spectra, and average biological response characteristics (ICRP, 2013; IAEA, 2018). The governing equation for AEDE determination is

$$AEDE(outdoor)(mSvy^{-1}) = D\ x\ 8760h\ x\ 0.7\ SvGy^{-1}x\ 0.2 \quad (9)$$

Where 8760 h is the number of hours in a year, 0.7 $SvGy^{-1}$ is the dose conversion coefficient from absorbed dose in air to effective dose for adults, and 0.2 represents the outdoor occupancy factor. AEDE is widely used to compare environmental exposure levels against regulatory limits (e.g., 1 mSv y^{-1} for the public) and to build spatial risk maps that reflect population dose burdens. It translates gamma survey data into a meaningful annual exposure quantity.

(d) Excess Life Cancer Risk

Excess lifetime cancer risk (ELCR), is the point at which radiation physics finally meets public health reality. While absorbed dose and effective dose tell us how much radiation energy reaches the body and how biologically significant that energy may be, ELCR translates those quantities into something people intuitively understand: the probability of developing cancer over the course of a lifetime as a result of that exposure. The concept begins with an important biological principle. At low and moderate environmental exposure levels, radiation induced cancer is considered a stochastic effect. This means that the severity of the disease does not increase with dose, but the probability of occurrence does. In other words, radiation does not guarantee cancer; instead, it slightly increases the chance that cancer may develop. This probability-based understanding is central to radiation protection frameworks developed by

international scientific bodies (UNSCEAR, 2016; ICRP, 2013). A standard formulation for ELCR based on annual effective dose is

$$ELCR = AEDE\ x\ DL\ x\ RF \quad (10)$$

Where AEDE is Annual Effective Dose Equivalent, DL is duration of life (usually assumed to be 70yrs), RF is the radiation risk factor (the detriment per unit dose, commonly taken as $0.05Sv^{-1}$ for the general public).

(v) Heavy Metal Toxicological Dose

The degree to which metals move from the environment into human tissues is controlled by several physical and chemical processes, including how a metal partitions between solid and liquid phases, how soluble it is under biological conditions, and how it crosses barriers like the skin or cell membranes (Brown and Walker 2013; Taylor et al. 2016).

Partitioning coefficients describe how a metal distributes between soil and water or between soil and skin. A high partitioning coefficient to soil means the metal prefers to stay attached to soil particles and is less available for uptake, whereas a high preference for water means it dissolves more readily and becomes more mobile. Bioaccessibility refers to how much of a contaminant dissolve in the fluids of the digestive tract and is therefore available for absorption. Once dissolved, the ability of a metal to enter cells depends on molecular diffusion and, for some species, active transport across membranes (Jones et al. 2017; Lee and Kim 2018).

Another key factor is metal speciation**,** the specific chemical form in which the metal exists. Speciation is controlled by environmental factors such as oxidation and reduction conditions. For example, chromium in its hexavalent form is stable under oxidizing conditions and can easily cross cell membranes, making it significantly more toxic and carcinogenic. By contrast, trivalent chromium forms strong complexes in soil and within organisms and is much less mobile and less biologically active (Green and Brown 2015; Wilson et al. 2018). Understanding these underlying physical and chemical behaviours helps toxicologists and risk assessors estimate how much of a metal might actually reach sensitive tissues and what health impacts that exposure could have.

Materials and Methods

Study Area

The Ariaria dumpsite is located in Ariaria town in Osisioma (the headquarters of the Osisioma/Ngwa Local Government Area of Abia State), is located along Aba–Port Harcourt Express way, about 500meters before Faulks Road junction. Osisioma is a semi-urban town, with a landmass198 Km^2 (76 Sq. miles) and a population of 219,632 (by the 2006 Nigeria Population Census data), with an average population density of 3500 inhabitants per square kilometer. Its coordinates are 5°8′59″N 7°19′49″E.

The vegetation in Ariaria is predominantly tropical rain forest. The soils are not much fertile and are prone to much leaching due to heavy rainfall. Trade and Agriculture are the major occupation of the people of the Area. The area covers a part of the popular Ariaria International Market and also possesses a rich alluvial soil which stretches through the study area. Commercial trading is prevalent and about 70% of the population engage in it while about 30% engages in subsistence farming. With its adequate seasonal rainfall, Ariaria has much arable land that produces yams, maize, plantains, and cassava. Rearing of livestock is also one of the prominent sectors of agriculture in the state.

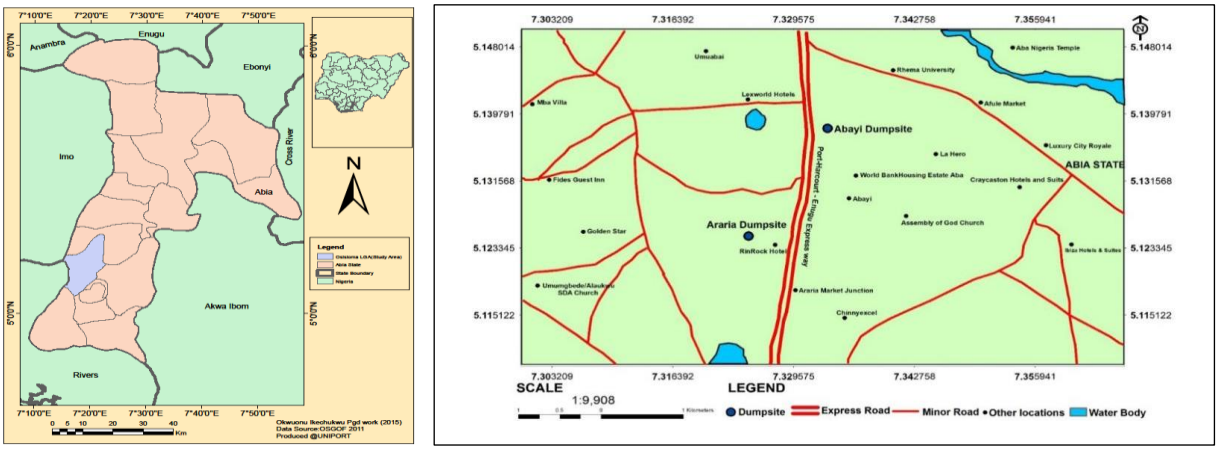

Fig. 1: Modified Google Map of the Study Area showing the Ariaria Municipal Waste Dumpsite

Radiological Parameters Experimental Procedure

In situ measurements were conducted around the Ariaria dumpsite. The *in-situ* approach of the gamma radiation measurement was chosen and adopted to enable samples maintain their original environmental characteristics. A digilert 200 nuclear radiation monitor meter (S.E international, INC. summer town, USA), containing a Geiger Muller tube with ionizing chamber which was pre- set to detect γ- radiation within a temperature range of -10 to 50^{O}C was applied for the gamma radiation measurement and a geographical positioning system (GPS) was used for the measurement of the point of sampling. The radiation meter's sensitivity was 3500 CPM/mRh^{-1} referenced to Cs-137 with a halogen-quenched Geiger-Muller detector tube of 45mm in diameter and a 1.5-2.0 $Mgcm^{-2}$ mica window density (Inspector Alert Operation Manual). During measurement, the tube of the radiation monitoring meter was raised to a standard height of 1.0m above the ground (Avwiri *et al.*, 2013) with its window facing the suspected source (products dispensing meters) at a distance of 5.0 m and the GPS values taken at the spot of radiation measurement. Readings were taken trice and average values obtained in accordance with NCRP recommendation (NCRP, 1993; Rafique *et al.*, 2014). The count rate per minute recorded in the meter was converted to milli-roentgen per hour (mRh^{-1}) using the relation (Avwiri *et al.*, 2013; Rafique *et al.*, 2014):

Count rate per minute (CMP) = 10^{-3} roentgen x Q.F (1)

Where Q.F is the quality factor, which is unity for external environment.

Heavy Metal Toxicological Analysis

Two grams of each sample were considered and oven dried at a temperature of 110˚C for a minimum of 4 hours. After cooling overnight, the samples were roasted at 850˚C in a furnace to eliminate extra air and moisture content, and then weighed once more. Six grams of X-ray flux were added to 0.7 grams of the dried samples, which had been measured into glass discs. This was done to lower the melting point of the samples and enable full homogenization. 35.3% lithium tetraborate (Li2B4O7) and 64.7% lithium metaborate (LiBO2) make up the X-ray flux. Care was taken when adding X-ray flux as observed by Willis and Duncan (2013) that flux should be dry and free of CO2, because many fluxes are hygroscopic, and can also adsorb CO2 from air. Thus, Platinum crucibles were employed in a gas fusion chamber to fuse the samples. By adding lithium bromide (LiBr), a releasing agent, the fused discs were also released from the platinum crucible in the gas fusion chamber. About 2.5g of LiBr was weighed and dissolved in 100 ml of water to help the samples come out of the crucible. Six drops of the dissolved releasing agent were then mixed

with the samples. During fusion (melting) the samples were subjected to a temperature of about 1100˚C in the chamber after which the samples were completely fused into a glass disc. After cooling, the discs were labeled and transferred into a desiccator. The fused discs were thereafter loaded into a Pananalytical AxiosmAX XRF Spectrometer chamber which is made of reinforced plastic and stainless steel. The automated lever system is connected to a clamp and rubber plate which picked the disc by suction, lower it into the stainless-steel loader while the clamp will grip the loader, lift it up and drop it into a hollow portion within the chamber that is in direct contact with the X-ray beam. It takes about 12 minutes for each sample to be analyzed. The lever system completes a cycle of operation by returning the sample disc to its original place. The XRF spectrometry operational settings was set at 4 kW, 60 kV (160 mA).

Results and Discussion

BIR at Ariaria Dumpsite

Table 1: BIR of Araria Dumpsite

Sample Codes	Geographical Coordinates		Exposure Rate(mR/h)			Average Radiation level (mR/h)	Absorbed dose (nGy/hr)	AEDE (mSv/y)	ELCR x 10^{-3}
	Latitude (N)	Longitude (E)	1st Rd	2nd Rd	3rd Rd				
ARR-1	5° 7'0.92"	7°20'13.51"	0.021	0.025	0.023	0.023	201.1	0.31	1.08
ARR-2	5° 7'0.67"	7°20'13.30"	0.026	0.020	0.018	0.021	185.0	0.29	0.99
ARR-3	5° 7'0.48"	7°20'13.05"	0.021	0.025	0.022	0.023	197.8	0.28	1.18
ARR-4	5° 7'0.92"	7°20'13.17"	0.025	0.029	0.023	0.026	220.1	0.34	1.18
ARR-5	5° 7'1.30"	7°20'13.35"	0.028	0.019	0.021	0.023	194.6	0.30	1.05
ARR-6	5° 7'1.47"	7°20'12.97"	0.025	0.022	0.017	0.021	185.0	0.29	0.99
ARR-7	5° 7'1.82"	7°20'12.74"	0.023	0.021	0.025	0.023	201.0	0.31	1.08
ARR-8	5° 7'1.34"	7°20'12.41"	0.029	0.021	0.019	0.023	194.6	0.30	1.05
ARR-9	5° 7'0.98"	7°20'12.71"	0.017	0.021	0.023	0.020	175.5	0.30	0.95
ARR-10	5° 7'1.32"	7°20'12.04"	0.025	0.021	0.019	0.022	188.2	0.29	1.01
ARR-11	5° 7'0.30"	7°20'12.67"	0.018	0.022	0.019	0.020	169.1	0.27	0.90
ARR-12	5° 7'0.87"	7°20'12.37"	0.026	0.021	0.018	0.022	188.2	0.29	1.01
ARR-13	5° 6'59.80"	7°20'10.45"	0.022	0.025	0.019	0.022	191.4	0.30	1.02
ARR-14	5° 7'0.17"	7°20'12.36"	0.024	0.027	0.021	0.024	210.5	0.32	1.13
ARR-15	5° 7'0.62"	7°20'11.88"	0.025	0.017	0.020	0.021	178.6	0.28	0.96
ARR-16	5° 7'0.88"	7°20'11.65"	0.027	0.021	0.023	0.024	207.4	0.32	1.11
ARR-17	5° 7'0.53"	7°20'11.46"	0.025	0.019	0.016	0.020	172.3	0.27	0.92
ARR-18	5° 6'59.81"	7°20'12.12"	0.028	0.021	0.019	0.023	194.6	0.30	1.05
ARR-19	5° 7'0.53"	7°20'11.18"	0.025	0.020	0.023	0.023	197.8	0.31	1.06
ARR-20	5° 7'0.15"	7°20'11.45"	0.020	0.023	0.021	0.021	185.0	0.29	0.99
ARR-21	5° 6'59.71	7°20'11.73"	0.021	0.018	0.023	0.021	178.6	0.28	0.96
ARR-22	5° 6'59.78"	7°20'11.39"	0.025	0.022	0.020	0.022	194.6	0.30	1.05
ARR-23	5° 7'0.09"	7°20'11.13"	0.024	0.023	0.019	0.024	210.5	0.29	1.13
ARR-24	5° 6'59.28"	7°20'11.45"	0.019	0.025	0.021	0.022	188.2	0.29	1.01
ARR-25	5° 7'0.03"	7°20'10.77"	0.025	0.022	0.029	0.025	220.1	0.34	1.18
ARR-26	5° 6'59.63"	7°20'10.95"	0.024	0.019	0.021	0.021	185.0	0.29	0.99
ARR-27	5° 6'59.61"	7°20'10.25"	0.022	0.025	0.019	0.022	191.4	0.30	1.02
ARR-28	5° 6'59.17"	7°20'11.11"	0.029	0.022	0.023	0.024	213.7	0.33	1.14
ARR-29	5° 6'59.21"	7°20'10.90"	0.023	0.020	0.018	0.020	175.5	0.26	0.95
ARR-30	5° 6'59.04"	7°20'10.46"	0.021	0.023	0.026	0.023	204.2	0.31	1.10
					AVERAGE	**0.022 ±0.001**	**193.3 ± 2.76**	**0.30 ±0.003**	**1.03 ±0.12**
					UNSCEAR, 2000	0.0133	89.0	1.0	0.29

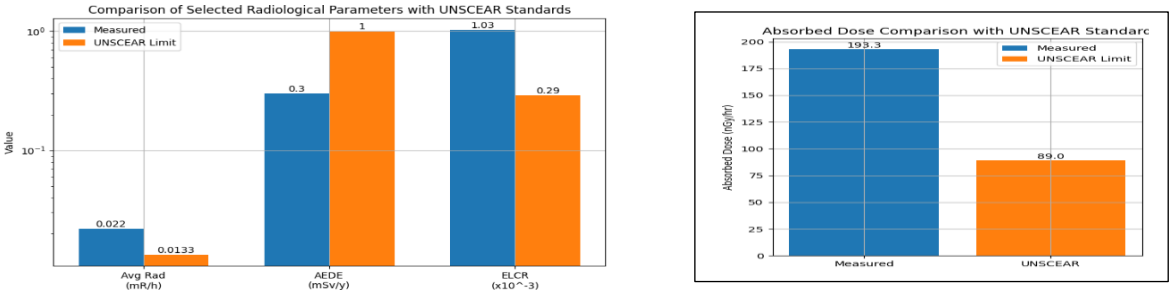

Fig. 2: Bar Charts comparing radiological parameters with UNSCEAR Standard

To improve visualization, absorbed dose was plotted separately due to its significantly higher magnitude compared to other radiological parameters. A logarithmic scale was applied to the combined plot of average radiation, annual effective dose equivalent and excess lifetime cancer risk. The results indicate that average radiation and excess lifetime cancer risk exceed United Nations Scientific Committee on the Effects of Atomic Radiation recommended limits, whereas the annual effective dose equivalent remains within permissible levels.

The measured background ionizing radiation (BIR) across the Ariaria dumpsite shows a relatively consistent spatial distribution, with average exposure rates clustering around 0.020–0.026 mR/h. The corresponding absorbed dose values (169.1–220.1 nGy/h; mean ≈ 193.3 nGy/h) are more than twice the global average value of 89 nGy/h recommended by the United Nations Scientific Committee on the Effects of Atomic Radiation. This elevation strongly suggests an enhancement of natural background radiation, most likely due to the accumulation of radionuclide-bearing wastes and prolonged anthropogenic inputs typical of open dumpsites.

The annual effective dose equivalent (AEDE), however, averages 0.30 mSv/y, which remains below the recommended public exposure limit of 1.0 mSv/y. This indicates that, from a strictly regulatory standpoint, the site does not yet pose an immediate radiological health hazard to the general population. Nonetheless, the excess lifetime cancer risk (ELCR), with a mean value of 1.03×10^{-3}, exceeds the global reference value of 0.29×10^{-3}. This is a critical finding because ELCR integrates long-term exposure effects and provides a more realistic indicator of cumulative health risk.

The observed discrepancy between acceptable AEDR and elevated ELCR reflects the chronic nature of low-dose radiation exposure in contaminated environments. Over time, even moderate radiation levels can lead to stochastic health effects, particularly carcinogenesis. The relatively high absorbed dose and ELCR values suggest that continuous exposure, especially for individuals living or working near the dumpsite, may increase the probability of radiation-induced cancers. The spatial variability observed across sampling points further indicates localized hotspots, likely linked to heterogeneous waste composition and uneven radionuclide distribution.

Table 2

Sample Codes	Sample Coordinates Latit(N)	Longit (E)	Heavy Metal Concentrations (PPM) Pb	Zn	Cd	Fe	Cr	As	Th	U	Cu	Ni	Co	Sn	
AR-01	5° 7'0.92"	7°20'13.51"	49.5	88	< 0.05	41910	286	11	15.6	4.39	32	112	43	32	
AR-02	5° 7'0.67"	7°20'13.30"	55	43	< 0.05	8900	320	13	17.4	5.91	57	78	67	28	
AR-03	5° 7'0.48"	7°20'13.05"	58	64	< 0.05	8690	78	12	14.8	6.01	36	63	35	31	
AR-04	5° 7'0.92	7°20'13.17"	63	78	< 0.05	9130	106	17	15.2	8.83	78	47	29	42	
AR-05	5° 7'1.30"	7°20'13.35"	48	79	< 0.05	15530	128	7	9.6	3.87	37	58	61	31	
AR-06	5° 7'1.47"	7°20'12.97"	47	84	< 0.05	5290	233	9	15.8	7.32	57	23	65	33	
AR-07	5° 7'1.82"	7°20'12.74"	62	88	< 0.05	15100	214	13	16.7	7.74	67	27	63	28	
AR-08	5° 7'1.34"	7°20'12.41"	53	74	< 0.05	9700	183	12	20.7	7.81	87	37	55	19	
AR-09	5° 7'0.98"	7°20'12.71"	48	77	< 0.05	10100	172	8	22.8	8.65	36	73	53	29	
AR-10	5° 7'1.32"	7°20'12.04"	51	83	< 0.05	11200	220	9	23.1	4.87	67	43	58	32	
AR-11	5° 7'0.30"	7°20'12.67"	53	66	< 0.05	15930	253	7	17.3	5.67	87	45	57	39	
AR-12	5° 7'0.87"	7°20'12.37"	46	65	< 0.05	11800	261	8	10.5	3.23	77	47	51	49	
AR-13	5° 6'59.80"	7°20'10.45"	45	59	< 0.05	8730	228	11	11.2	5.23	57	31	45	37	
AR-14	5° 7'0.17"	7°20'12.36"	57	63	< 0.05	8320	219	13	9.8	4.32	65	33	52	38	
AR-15	5° 7'0.62"	7°20'11.88"	52	64	< 0.05	7130	231	17	13.9	6.15	43	47	48	42	
AR-16	5° 7'0.88"	7°20'11.65"	51	79	< 0.05	14300	108	7	12.3	5.21	45	87	23	39	
AR-17	5° 7'0.53"	7°20'11.46"	43	72	< 0.05	15200	117	9	14.2	2.65	46	93	19	43	
AR-18	5° 6'59.81"	7°20'12.12"	47	73	< 0.05	10100	121	8	10.3	3.52	46	94	47	34	
AR-19	5° 7'0.53"	7°20'11.18"	53	75	< 0.05	11100	133	12	18.1	3.76	57	92	67	39	
AR-20	5° 7'0.15"	7°20'11.45"	52	76	< 0.05	1210	142	13	23.9	3.59	63	93	63	41	
AR-21	5° 6'59.71	7°20'11.73"	51	85	< 0.05	6700	121	14	26.1	4.32	51	91	52	37	
AR-22	5° 6'59.78"	7°20'11.39"	64	83	< 0.05	7300	123	14	8.8	5.36	36	58	53	33	
AR-23	5° 7'0.09"	7°20'11.13"	63	75	< 0.05	8300	108	9	13.5	6.13	43	53	57	23	
AR-24	5° 6'59.28"	7°20'11.45"	65	66	< 0.05	4800	109	9	14.2	5.25	51	51	57	32	
AR-25	5° 7'0.03"	7°20'10.77"	61	68	< 0.05	41300	118	11	14.1	3.21	38	34	53	21	
AR-26	5° 6'59.63"	7°20'10.95"	43	53	< 0.05	42100	112	13	15.3	3.47	53	45	51	43	
AR-27	5° 6'59.61"	7°20'10.25"	47	62	< 0.05	38100	121	8	16.2	4.34	35	43	45	23	
AR-28	5° 6'59.17"	7°20'11.11"	46	63	< 0.05	32100	107	19	19.1	5.29	47	49	37	43	
AR-29	5° 6'59.21"	7°20'10.90"	64	71	< 0.05	3120	164	17	23.7	6.12	47	51	39	39	
AR-30	5° 6'59.04"	7°20'10.46"	61	76	< 0.05	38700	157	13	25.1	5.37	53	35	43	41	
Average			**53.3**	**71.7**	**< 0.05**	**1539.3**	**166.4**	**11.4**	**16.3**	**5.3**	**53.1**	**57.8**	**49.6**	**34.7**	

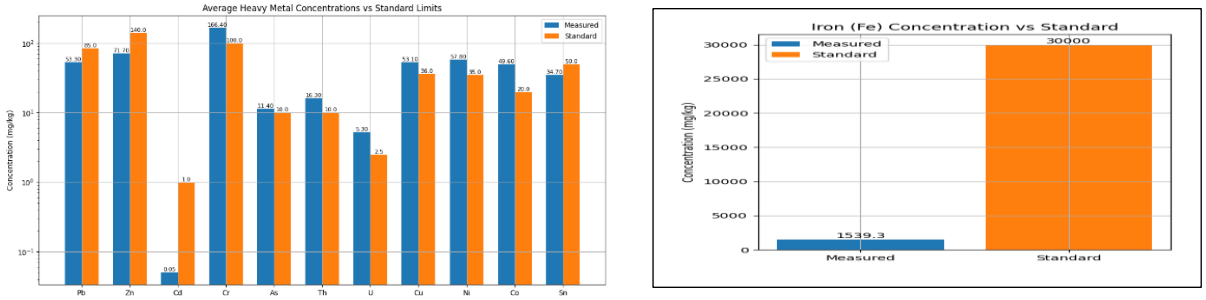

Fig. 3: Log Scale Bar Chart comparing the Concentrations of Heavy Metals with Standards

A logarithmic scale bar chart was used to compare the average concentrations of heavy metals with established guideline values from World Health Organization, United States Environmental Protection Agency and Department of Petroleum Resources. Iron was plotted separately due to its relatively high background concentration. The results indicate that chromium, uranium, thorium, nickel and cobalt exceed recommended limits, suggesting moderate contamination. In contrast, cadmium, lead, zinc and arsenic remain within permissible limits, indicating lower environmental risk from these metals.

The geochemical analysis reveals a complex contamination profile, with varying degrees of enrichment across different heavy metals. Mean concentrations show that iron (Fe) dominates the elemental composition, reflecting its natural abundance in soils. However, more environmentally significant are the elevated levels of chromium (Cr), thorium (Th),

uranium (U), nickel (Ni), and cobalt (Co), all of which exceed recommended limits set by regulatory agencies such as the World Health Organization and the United States Environmental Protection Agency.

Chromium concentrations (mean ≈ 166.4 ppm) are particularly concerning due to the potential presence of hexavalent chromium (Cr^{6+}), a highly toxic and carcinogenic species. Similarly, elevated uranium and thorium levels indicate the presence of naturally occurring radioactive materials (NORM), which may contribute to both chemical toxicity and radiological exposure. Nickel and cobalt, which also exceed permissible limits, are known for their mutagenic and carcinogenic properties, especially under prolonged exposure.

In contrast, cadmium (Cd), lead (Pb), zinc (Zn), and arsenic (As) remain within permissible limits, suggesting that their contribution to overall toxicity is currently limited. However, it is important to recognize that even metals within regulatory thresholds can become hazardous through bioaccumulation and synergistic interactions in the food chain.

The spatial distribution of these metals suggests strong anthropogenic influence, likely from mixed municipal, industrial, and electronic waste streams. The variability in concentrations across sampling points reflects differences in waste composition, leachate migration, and soil geochemistry. The presence of elevated Fe alongside trace metals also points to possible redox-controlled mobilization processes, which can enhance the bioavailability of toxic elements under changing environmental conditions.

Conclusion

This study has shown that the co-occurrence of elevated radiological parameters and heavy metal contamination at the Ariaria dumpsite presents a compounded environmental health concern. While each class of pollutant poses its own risks, their interaction can lead to synergistic effects that amplify overall toxicity. Moreover, the presence of uranium and thorium introduces a dual hazard, as these elements contribute both to internal radiation exposure and chemical toxicity. This duality complicates risk assessment, as traditional models often treat radiological and chemical risks independently. In reality, populations exposed to such environments experience simultaneous multi-pathway exposure through inhalation of dust, ingestion of contaminated soil or water, and dermal contact.

The findings reveal that the Ariaria dumpsite represents a moderately contaminated environment with clear evidence of anthropogenic impact. Although individual parameters such as AEDE remain within permissible limits, the elevated absorbed dose, ELCR, and concentrations of key toxic metals point to a chronic exposure scenario with potential long-term health implications. This underscores the need for integrated environmental monitoring, risk mitigation strategies, and possible remediation efforts to reduce both radiological and chemical hazards in the area.

References

Abayiga, A. N., Gbarato, O. L., & Biibaloo, L. L. (2024). Assessment of background ionizing radiation levels at selected dumpsites in Obio/Akpor Local Government Area, Rivers State, Nigeria. *Faculty of Natural and Applied Sciences Journal of Applied and Physical Sciences,* 2(2), 39-48.

Adeleke, A. T., Odunaike, R. K., Alausa, S. K., Olayiwola, I. O., Talabi, A. T., Adeniji, Q. A., & Adeniyi, A. C. (2024). Heavy metals analysis and physicochemical characterization of groundwater at a battery recycling site in southwestern Nigeria. *Tanzania Journal of Science, 49*(5), 1097–1109.

Afon, A. O., Olorunfemi, F. B., & Akinyemi, O. (2017). Environmental risk assessment of heavy metals near municipal solid waste dumpsites in Nigeria. *Environmental Monitoring and Assessment, 189*(9), 465-476.

Alloway, B. J. (2013). *Heavy metals in soils: Trace metals and metalloids in soils and their bioavailability* (3rd ed.). Springer.

ATSDR (Agency for Toxic Substances and Disease Registry). (2012). *Toxicological profile for chromium*. U.S. Department of Health and Human Services.

Avwiri, G.O., Egieya, J. F., and Chinyere, P. O. (2013). Radiometric survey of Aluu landfill in Rivers State, Nigeria. *Adv. Phys. Theories Appl.* 22, 24-30.

Bradl, H. B. (2017). Heavy metal sorption and mobility in soils. *Environmental Chemistry Letters, 15*(3), 417–432.

Brown, A. L., & Walker, S. R. (2013). Environmental partitioning and human exposure to trace metals. *Environmental Toxicology Journal, 28*(4), 301–312.

Chen, G., & Wang, X. (2018). Influence of soil properties on heavy metal transport and retention. *Journal of Contaminant Hydrology, 210*, 1–12.

Christensen, T. H., Kjeldsen, P., Bjerg, P. L., Jensen, D. L., Christensen, J. B., Baun, A., Albrechtsen, H. J., & Heron, G. (2011). Biogeochemistry of landfill leachate plumes. *Applied Geochemistry, 26*(11), 1599–1615.

Echeweozo, E. O., Nworie, C. I., Ojobeagu, A. O., Otah, P. B., & Okoro, I. J. (2025). Health risk assessment due to environmental radioactivity and heavy metal contamination at the central solid waste dumpsite in Ebonyi State, Nigeria. *Journal of the Nigerian Society of Physical Sciences, 7*(2), 2160-2173.

Ezeonu, C. S., Nwadinigwe, A. O., & Ozoh, P. T. E. (2018). Microbial contamination of groundwater sources near municipal solid waste dumpsites in southeastern Nigeria. *Environmental Monitoring and Assessment, 190*(8), 474.

Ferronato, N., & Torretta, V. (2019). Waste mismanagement in developing countries: A review of global issues. *International Journal of Environmental Research and Public Health, 16*(6), 1060-1071.

Fischer, T., & Kincaid, C. (2014). Advective and dispersive mechanisms controlling contaminant migration. *Groundwater Monitoring & Remediation, 34*(3), 48–59.

Green, D. M., & Brown, P. E. (2015). Redox chemistry and bioavailability of chromium species in soil and water. *Journal of Hazardous Materials, 298*, 102–111.

Gworek, B., Dmuchowski, W., Baczewska-Dąbrowska, A. H., & Gołębiowska, D. (2018). Environmental pollution by compounds emitted from municipal waste landfills. *Environmental Monitoring and Assessment, 190*(1), 1–17.

Ilechukwu, I., Ayoade, O., & Onwuemesi, A. (2020). Heavy metal contamination of soils around open dumpsites in southeastern Nigeria and associated ecological risks. *Environmental Challenges, 1*, 100007.

Hubbard, S. S., & Auken, E. (2015). Geophysical imaging of subsurface processes for contamination mapping. *Reviews of Geophysics, 53*(3), 297–337.

International Atomic Energy Agency (2013). *Management of NORM residues* (IAEA-TECDOC-1712). International Atomic Energy Agency, Vienna, Austria. ISBN 978-92-0-142710-6.

International Atomic Energy Agency. (2014). *Radiation dose assessment models for environmental exposure*. IAEA, Vienna, Austria. ISBN 978-92-0-113714-1.

International Atomic Energy Agency (2018). *Quantifying environmental external exposure from natural radiation sources*. International Atomic Energy Agency, Vienna, Austria. ISBN 978-92-0-101718-8.

International Commission on Radiological Protection. (2013). Radiological protection in geological disposal of long lived solid radioactive waste. ICRP Publication 122. Annals of the ICRP, 42(3).

Izquierdo, M., & Querol, X. (2012). Leaching behaviour of elements from coal combustion fly ash: An overview. *International Journal of Coal Geology, 94*, 54-66. Elsevier B.V.

Jones, B. H., Richards, T. A., & Miller, S. D. (2017). Bioaccessibility of metals in dust and soils and implications for exposure. *Science of the Total Environment, 575*, 73–82.

Kaza, S., Yao, L., Bhada-Tata, P., & Van Woerden, F. (2018). *What a Waste 2.0: A global snapshot of solid waste management to 2050*. World Bank.

Knoll, G. F. (2010). *Radiation detection and measurement* (4th ed.). John Wiley & Sons.

Kosson, D. S., van der Sloot, H. A., Sanchez, F., & Garrabrants, A. C. (2002). An integrated framework for evaluating leaching in waste management and utilization of secondary materials. *Environmental Engineering Science, 19*(3), 159–204.

Kosson, D. S., Garrabrants, A. C., DeLapp, R., van der Sloot, H. A., & Sanchez, F. (2014). *Leaching Environmental Assessment Framework (LEAF): Overview and applications*. U.S. Environmental Protection Agency, Office of Research and Development, Washington, DC, USA. EPA/600/R-14/061.

Kosson, D. S., van der Sloot, H. A., Sanchez, F., & Garrabrants, A. C. (2014). An integrated framework for evaluating leaching in waste management and utilization of secondary materials. *Environmental Engineering Science, 31*(7), 379–393.

Landrigan, P. J., Fuller, R., Acosta, N. J. R., et al. (2018). The Lancet Commission on pollution and health. *The Lancet, 391*(10119), 462–512.

Lee, J. Y., & Kim, H. J. (2018). Dermal absorption and transport mechanisms of heavy metals. *Toxicology Letters, 286*, 156–165.

Li, J., & Zhang, Y. (2016). Mobility of trace metals in groundwater influenced by redox conditions. *Environmental Earth Sciences, 75*, 990.

McLaughlin, J. B., Smith, A. B., & Jones, C. D. (2013). Field characterization of gamma radiation spatial footprints for in-situ dose rate measurements. *Journal of Environmental Radioactivity, 115*, 12–24.

Meima, J. A., & Comans, R. N. J. (1998). Geochemical modeling of weathering reactions in municipal solid waste incinerator bottom ash. *Environmental Science & Technology, 32*(5), 688–693.

Nanda, S., & Berruti, F. (2021). Municipal solid waste management and landfilling technologies: A review. *Environmental Chemistry Letters, 19*(2), 1433–1456.

National Council on Radiation Protection and Measurements (NCRP). 1993. Limitation of exposure to ionizing radiation, NCRP Report No. 116. (March Nobel, BJ. 1990). An introduction to radiation protection, Macmillan family Encyclopedia. (2nd edi.). 16-118.

Owamah, H. I., Alfa, M. I., & Akudo, E. U. (2020). Groundwater contamination from dumpsite leachate in a Nigerian city: Implications for public health. *Environmental Quality Management, 29*(3), 55-66.

Oyebamiji, A. O., Egirani, D. E., & Awofolu, O. R. (2019). Spatial variation, contamination levels, and health risk assessment of heavy metals in soils around a dumpsite in southwestern Nigeria. *Journal of African Earth Sciences, 156*, 142-51.

Prüss-Ustün, A., Wolf, J., Corvalán, C., Bos, R., & Neira, M. (2019). Preventing disease through healthy environments: A global assessment of the burden of disease from environmental risks. *WHO Bulletin, 97*(4), 224–244.

Rafique, M., Saeed, U. R., Muhammad, B., Wajid, A., Iftikhar, A., Khursheed, A. L. and Khalil, A. M. (2014). Evaluation of excess life time cancer risk from gamma dose rates in Jhelum Valley. *Journal of Radiation Research and Applied Science,* 7, 29-35.

Smith, K. E., & Jones, M. L. (2015). Human behavior in environmental radiation exposure assessment. *Journal of Radiological Protection, 35*(2), 321–338.

Tollefson, D. A., Richards, P. L., & Holloway, D. M. (2015). Influence of soil moisture and density on environmental gamma ray measurements. *Radiation Physics and Chemistry, 117*, 179–186.

Ugwuaji, J. O., Ezeugwu, U. L., & Omorodion, F. U. (2015). Spatiality, seasonality and ecological risks of heavy metals around a municipal dumpsite in Enugu, Nigeria. *Journal of Environmental Health Science and Engineering, 13*(15).

UN Environment Programme. (2019). *Waste management outlook for Africa*. UNEP. https://www.unep.org/resources/report/waste-management-outlook-africa.

United States Environmental Protection Agency (2014). *Coal Combustion Residual Beneficial Use Evaluation: Fly Ash Concrete and FGD Gypsum Wallboard* (EPA530-R-14-001). U.S. Environmental Protection Agency, Office of Solid Waste and Emergency Response, Washington, DC, USA. https://www.epa.gov/sites/default/files/2014-12/documents/ccr_bu_eval.pdf.

United Nations Scientific Committee on the Effects of Atomic Radiation. (2000). *Sources and effects of ionizing radiation: UNSCEAR 2000 report to the General Assembly, with scientific annexes* (Volumes I & II). United Nations. ISBN 92-1-142238-8 (Vol. I); 978-9211422399 (Vol. II).

United Nations Scientific Committee on the Effects of Atomic Radiation (2016). *Sources, effects and risks of ionizing radiation: UNSCEAR 2016 Report, Volume I*. United Nations Scientific Committee on the Effects of Atomic Radiation, United Nations, New York, NY, USA. ISBN 978-92-1-142440-6.

Wilson, D. C., Rodic, L., Scheinberg, A., Velis, C. A., & Alabaster, G. (2015). Comparative analysis of solid waste management in 20 cities. *Waste Management & Research, 33*(9), 813–826.

Wilson, R. J., Patel, S. N., & Thompson, C. A. (2018). Comparative toxicity of chromium species in human cells. *Environmental Research, 164*, 323–330.